# Semiclassical theory of spectral line shapes. II. Applications to CO, HCl, and OCS, broadened by inert gases\*

D. E. Fitz and R. A. Marcus

Department of Chemistry, University of Illinois, Urbana, Illinois 61801 (Received 23 January 1975)

The semiclassical theory of spectral line broadening developed in the previous paper of this series is used to calculate the half-widths and shifts of nonoverlapping rotational spectral lines of CO, HCl, and OCS, broadened by inert gases. Comparisons are made with the available experimental data and with related theoretical analyses, and reasonable agreement is obtained. The method used applies both to fairly quantum systems as well as to the relatively classical ones. A symmetrized semiclassical expression for Wigner 6-j symbols is given and applied.

#### I. INTRODUCTION

The effect of collisions on molecular spectral line shapes has been calculated by a variety of perturbative and nonperturbative methods. <sup>1</sup> In the present paper we apply the semiclassical theory of the linewidths and shifts developed in the preceding paper of this series <sup>2</sup> (hereafter referred to as Part I). These first applications are made to the CO-He, HCl-He, HCl-Ar, OCS-He, and OCS-Ar systems, <sup>3</sup> each of which has been extensively studied and for each of which a potential energy function is available. <sup>4,5</sup>

The CO, OCS, and HCl-He systems have been treated by a classical-type method by Gordon, 4 who calculated linewidths. 6,7 Using instead a classical path method, widths and shifts have been calculated for the HCl-Ar system by Neilsen and Gordon. 5 This latter method assumed a zeroth order decoupling of the relative translational and internal motions, of which the former was treated by classical mechanics and the latter by timedependent quantum mechanics for the coupled internal states. Although this second method was called semiclassical, it is not to be confused with "semiclassical" as used in the present series. It has been suggested<sup>8</sup> that the HCl-Ar system is best treated using the classical path method for the low rotational angular momenta and the classical method for the higher ones. The present paper investigates the use of the semiclassical method for both cases for this and the other systems.

During the course of many studies on the collisional broadening of spectral lines, three collisional effects occur, and at least some have been included in each of those studies. These effects are collisional deactivation, collisionally induced phase shift of the molecular motion of the absorber, and collisionally induced reorientation of that rotating molecule (absorber). The first of these effects has a major effect on the linewidth, while the second has a major effect on the line shift, and the third has some influence on both. A helpful discussion of all three has been given by Gordon in his classical-like analysis. 4

All three of these effects occur automatically in the semiclassical theory, and that aspect of the relation between that theory and the classical theory of Gordon was discussed in Part I. In the present paper, numerical results are obtained, compared with the experimental

 $data^{9-11}$  and with the previous theoretical results in Refs. 4 and 5.

One minor difference from Part I, apart from the typographical and other corrections given in Appendix A, is the introduction of a symmetrized semiclassical expression for the Wigner 6-j symbol, which is used to replace the less symmetrical one given in Edmonds.  $^{12,2}$  A comparison of the two with the exact values of these coefficients is given later in Table I.

# II. METHODOLOGY

The reduced line shape expression for nonoverlapping rotational lines is the familiar Lorentzian, one with a negative-resonance term, given in Part I as

$$I(\omega) = \frac{1}{\pi} \operatorname{Im} \left| \left\langle j_f \parallel \mu \parallel j_i \right\rangle \right|^2$$

$$\times \left[ \frac{\rho_i}{\omega - \omega_0 - d - iw} + \frac{\rho_f}{\omega + \omega_0 + d - iw} \right]$$
 (2.1)

where  $I(\omega)$  is the reduced line shape; Im denotes "imaginary part of";  $j_i$  and  $j_f$  denote the initial and final rotational quantum numbers, respectively;  $\mu$  is the dipole moment operator in a term which is the reduced matrix element of  $\mu$ ;  $\rho_i$  and  $\rho_f$  are the normalized Boltzmann density distributions of  $j_i$  and  $j_f$ , apart from the relevant degeneracies<sup>13</sup>;  $\omega$  is the angular frequency of the incident radiation;  $\omega_0$  is the angular frequency corresponding to the transition  $j_i \rightarrow j_f$ ; and w and d are half-width and shift of the line  $j_i \rightarrow j_f$ , respectively. The latter are defined by the real and imaginary parts of a velocity-weighted ensemble-averaged collision cross section:

$$w = N \operatorname{Re} \langle v \sigma_{if,if} \rangle ,$$

$$d = -N \operatorname{Im} \langle v \sigma_{if,if} \rangle ,$$
(2. 2)

where N is the number density of the perturbers, i and f denote  $j_t$  and  $j_f$ , and where

$$\langle v\sigma_{if,if}\rangle = \int_{0}^{\infty} v\sigma_{if,if}(v)\rho_{v}dv$$
 (2.3)

Here, v is the relative velocity of the perturbing atom and the rotor and  $\rho_v$  is the Maxwell-Boltzmann distribution function

$$\rho_{v} = (\mu/2\pi k_{B}T)^{3/2} 4\pi v^{2} \exp(-\mu v^{2}/2k_{B}T) , \qquad (2.4)$$

where  $\mu$  is the reduced mass of the atom-diatom pair,  $k_B$  is Boltzmann's constant, and T is the temperature of the system of interest.

The general quantum mechanical form of a generalized collision cross section  $\sigma_{i'f',if}^{K}$  for an atom-rigid rotor system is<sup>1,2</sup>

$$\sigma^{K}_{i*f^{\bullet},if} = \frac{\pi}{k^{2}} \sum_{li^{\bullet}J_{i}J_{f}} (-1)^{i-l^{\bullet}+j_{i}-j_{i}^{\bullet}} (2J_{i}+1)(2J_{f}+1) \begin{cases} J_{f} & J_{i} & K \\ j_{i} & j_{f} & l \end{cases} \begin{cases} J_{f} & J_{i} & K \\ j_{i}^{\bullet} & j_{f}^{\bullet} & l^{\bullet} \end{cases} \left[ \delta_{j_{i}^{\bullet}j_{f}^{\bullet}} \delta_{j_{f}^{\bullet}j_{f}^{\bullet}} \delta_{j_{f}^{\bullet}j_{f}^{\bullet}} \delta_{l^{\bullet}i} - S_{j_{i}^{\bullet}i_{f}^{\bullet}i_{f}^{\bullet}j_{f}^{\bullet}}^{*}(E_{i}) S_{j_{f}^{\bullet}i_{f}^{\bullet}i_{f}^{\bullet}j_{f}^{\bullet}}^{*}(E_{f}) \right],$$

$$(2.5)$$

where the subscript i's and f's denote the quantities before and after interaction with the radiation, respectively; unprimed and primed variables represent preand post-collisional quantities; j's, l's, and J's represent the appropriate rotational, orbital, and total quantum numbers; the terms in braces are Wigner 6-i symbols; K is the tensorial order of the interaction with the radiation, and is unity for dipolar microwave spectra; k is the wavenumber of the relative motion between the atom and diatom; and S denotes the scattering S matrix. The assumptions used in deriving (2.1), (2.3), and (2.5) were (i) the system is dilute enough in absorber molecules that absorber-absorber interactions may be neglected, (ii) the system is at sufficiently low pressures that the approximation of uncorrelated binary absorberperturber molecular collisions and distribution functions may be used, and (iii) most importantly, the impact approximation is valid.

The details of the transformation of (2.5) into its semiclassical form were given in Part I. The assumptions made in this transformation were the following: (i) use of a primitive semiclassical form of the S matrix, or some uniform version when necessary, (ii) sums in (2.5) over the quantum numbers l, l', and  $J_l$ may be converted into integrals so that a partial averaging technique14 may be utilized, (iii) use of a semiclassical-like expression for the Wigner 6-i symbol, given by Eq. (2.6) below. There is also an approximation used analogous to that used in the normalization of the primitive semiclassical wavefunctions in general: The preexponential factors of the two semiclassical S matrices are replaced by a common one which uses an average j, J, and E, and the phases of those two S matrices are expanded about this average j, J, and E, retaining only the linear terms in the expansion. This approximation of course works better the closer the collision dynamics of the  $j_i$  and  $j_f$  states. The symbols  $\hat{j}_i$ ,  $\hat{l}$ , and  $\hat{J}_i$  will be used to denote  $\hat{j}_i + \frac{1}{2}$ ,  $l + \frac{1}{2}$ , and  $\hat{J}_i + \frac{1}{2}$ , and  $\hbar$  is set equal to unity. The arithmetic mean of  $\hat{j}_i$ and  $\hat{j}_f$  and that of  $\hat{J}_i$  and  $\hat{J}_f$  are denoted by  $\hat{j}$  and  $\hat{J}_i$ , respectively.

An expression is available in the literature for the 6-j symbol valid for the case where five of the six angular momenta are large relative to the sixth. <sup>12</sup> In the present case, three of the angular momenta,  $J_t$ ,  $J_f$ , and l, are usually large, while K is unity,  $j_f$  is  $j_{i\pm 1}$ , and  $j_i$  is usually small. A semiclassical expression, obtained by symmetrizing the one given in Part I, is

$$\begin{cases}
J_f J_i K \\
j_i j_f l
\end{cases} \cong (-1)^{i+j_i+J_{f+K}} [(j_i+j_f+1)(J_i+J_f+1)]^{-1/2} d_{0\lambda}^K(\xi) ,$$
(2.6)

where  $\lambda = J_f - J_i$ ,  $\delta = j_f - j_i$ , and  $\xi$  is the angle between the classical variables j and J shown in Fig. 1 and is given by given by

$$\cos \xi = (\hat{J}^2 + \hat{j}^2 - \hat{l}^2)/2\hat{j}\hat{J} \quad . \tag{2.7}$$

The expression in Part I, which had  $(2j_i+1)(2J_i+1)$  instead of  $(j_i+j_f+1)(J_i+J_f+1)$ , was prompted by the expression in Edmonds<sup>12</sup> for the case of five large momenta. Equation (2.6) satisfies the relevant symmetry relations<sup>15</sup> exactly, while that in Edmonds satisfies some of them only approximately (see Footnote b in Table I given later). The comparison with exact values for the 6-j symbols is given later.

The semiclassical expression for the  $\sigma_{i^*f^*,if}^K$  in (2.5) is as obtained in Part I, apart from a few changes which are described in Appendix A of the present paper. We have, thereby,

$$\sigma_{i \neq f^{\bullet}, i \neq f}^{K} = 2\pi \int_{0}^{\infty} b db \ S(b) \quad , \tag{2.8}$$

where i'f', if denotes  $j'_ij'_f$ ,  $j_ij_f$ ; b is the impact parameter

$$b = \hat{t}/\mu v \tag{2.9}$$

 $(\hbar = 1)$ ; and

$$S(b) = \delta_{i'i}\delta_{f''f} - \int_{|\hat{J}-\hat{I}|}^{\hat{J}+\hat{I}} d\hat{J}(\hat{J}/2\hat{J}\hat{I}) \int_{0}^{\pi} (d\bar{q}_{1}/\pi)P_{\hat{J}',\hat{J}}, \quad (2.10)$$

TABLE I. Quantum and approximate values of some 6-j symbols.<sup>a</sup>

$J_f$	$J_{l}$	$K:j_{l}$	$j_f$	ı	Quantum	Approximation Present	Approximation Refs. 12, 2
11	11	0:2	2	12	-0.0933	-0.0933	-0.0933
3	2	1:1	2	2	-0.1633	-0.1595	-0.1443
2	3	1:1	0	2	0.2582	0.2345	0.1982
6	5	1:5	4	8	0.0545	0.0542	0.0542
8	9	1:4	5	12	-0.0583	-0.0581b	-0.0590b
4	5	1:8	9	12	-0.0583	-0.0581b	-0.0578b
11	9	2:4	6	12	-0.0113	-0.0123	-0.0040(!)
11	9	2:2	4	11	0.0129	0.0155	0.0013(!)
9	7	2:5	7	8	0.0318	0.0321b	0.0267b
5	7	2:9	7	8	0.0318	0.0321b	0.0342b

 $<sup>\</sup>begin{bmatrix} \mathbf{a} & \left\{ \begin{matrix} J_f & J_l & \mathbf{K} \\ j_l & j_f & l \end{matrix} \right\},$ 

where  $j_i$ ,  $j_f$ , and K are typically, though not necessarily, chosen to be smaller than  $J_i$ ,  $J_f$ , and l.

<sup>b</sup>Although the approximations in the last two columns satisfy the symmetry relation

only the present approximation satisfies the symmetry relation

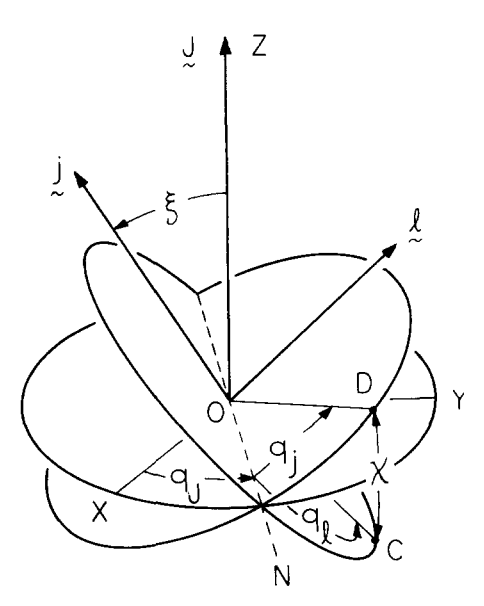


FIG. 1. Internal coordinates  $q_j$ ,  $q_l$ , and  $q_J$  for the motion of an atom and rigid rotor. The rotor axis lies along OD and the line of centers of the collision partners lies along OC at any instant of time.

where  $P_{\hat{j},\hat{j}}$  is a transition probabilitylike quantity, whose primitive semiclassical value is (using the geometric mean approximation referred to earlier)

$$P_{\hat{j}^{\bullet},\hat{j}}(\overline{q}_{j},\hat{J},\hat{j},\hat{l}) = s \sum_{\mathbf{S},\mathbf{p}_{\bullet}} \left| \partial \hat{j}' / \partial (\overline{q}_{j}/2\pi) \right|^{-1} D_{\delta^{\bullet}\delta}^{K}(\alpha\beta\gamma) . \tag{2.11}$$

In these equations, primes denote post-collision quantities, as before; the coordinates canonically conjugate to  $\hat{j}$ ,  $\hat{l}$ , and  $\hat{J}$ , and  $P_R$  are  $q_j$ ,  $q_l$ ,  $q_J$ , and R (the separation distance), the angles being those described in Fig. 1;  $\delta$  denotes  $j_f - j_i$ ; for the present system of non-overlapping lines,  $\delta = \delta' = 1$  and K = 1;  $\overline{q}_l$  and  $\overline{q}_j$  are constants defining initial conditions of a trajectory and are equal to  $q_l$  and  $q_j - R\omega_j/v$ , respectively, at large enough R; expressions at smaller R are given in Appendix B;  $\omega_j$  is the angular rotational frequency.  $\Sigma$  denotes a sum over stationary phase points (s.p.).

The interaction potential will be denoted by  $V(R,\chi)$ , where  $\chi$  is the angle between the axis of the rotor and the line of centers of the collision partners. When  $V(R,\chi)$  equals  $V(R,\pi-\chi)$ , one finds (Appendix B) that the  $\Sigma$  is over a  $\pi^2$  interval in  $(\overline{q}_1,\overline{q}_j)$  space and s=4. When the potential does not have that property and when any interferences between the  $(0,\pi)$  and  $(\pi,2\pi)$  intervals of  $\overline{q}_j$  space are neglected, the sum over stationary phase points is over a  $\pi$  interval of  $\overline{q}_1$  and a  $2\pi$  interval of  $\overline{q}_j$ , and then s=1 (Appendix B), i.e.,

$$\sum_{\mathbf{s},\mathbf{p},} = \sum_{\mathbf{r}^2}, \quad s = 4 \quad [V(\chi) = V(\pi - \chi)]$$

$$\sum_{\mathbf{s},\mathbf{p},} = \sum_{\mathbf{r}^2}, \quad s = 1 \quad \text{(otherwise)} \quad .$$
(2.12)

For the first line in (2.12), one finds that  $\delta$  and  $\delta'$  can differ at most by an even integer (Appendix B), and one also obtains the selection rule  $j'_i - j_i =$  an even integer. In Eq. (2.11),  $D^{\kappa}_{\delta'\delta}(\alpha\beta\gamma)$  denotes an expression given by

Eq. (C6) in terms of  $\xi$ ,  $\xi'$ , and several other quantities. It also proves to be a rotation matrix (Appendix C), where  $\beta$  is the angle between j and j', and is given by Eq. (2.13);  $\alpha$  and  $\gamma$  are phase shift angles defined by (2.14) and (2.15) and described in Fig. 2:

$$\cos\beta = \cos\xi \cos\xi' + \sin\xi \sin\xi' \cos(q_J' - q_J) , \qquad (2.13)$$

 $\tan\left[\alpha - (q_j' - \omega_j' t')\right] = \sin\xi' \sin(q_J' - q_J) / [\cos\xi \sin\xi']$ 

$$-\sin\xi\cos\xi'\cos(q_J'-q_J)], \qquad (2.14)$$

 $\tan[\gamma - (q_j - \omega_j t)] = \sin\xi' \sin(q_J' - q_J) / [-\cos\xi' \sin\xi]$ 

$$+\sin\xi'\cos\xi\cos(q_J'-q_J)$$
 . (2.15)

Both  $\alpha-(q_j'-\omega_j't')$  and  $\gamma-(q_j-\omega_jt)$  lie in the  $(0,2\pi)$  interval, the quadrant in each case being determined from the signs of both the numerator and the denominator on the right hand sides of (2.14)-(2.15). The angle  $\beta$  lies in the  $(0,\pi)$  interval, the angle  $\xi$  in (2.13)-(2.15) is given by (2.7), and  $\xi'$  is given by a similar relationship. The angles  $q_j'-\omega_j't'$  and  $q_j-\omega_jt$  are denoted by q' and  $q_j$ , respectively, in Fig. 2. (In Ref. 16a they are denoted by  $\tilde{q}_j'$  and  $\tilde{q}_j$ .)

Equations (2.8)-(2.11) have a relatively simple physical interpretation:  $2\pi bdb$  is the probability that the impact parameter lies in (b,b+db);  $\hat{J}d\hat{J}/2\hat{\jmath}\hat{l}$  is the probability that  $\hat{J}$  lies in  $(\hat{J},\hat{J}+d\hat{J})$  for a given  $\hat{\jmath}$  and  $\hat{l}$  (i. e., b);  $d\bar{q}_I/2\pi$  is the probability that  $\bar{q}_I$  lies in  $(\bar{q}_I,\bar{q}_I+d\bar{q}_I)$ ; and  $P_{\hat{\jmath}',\hat{\jmath}}$  is a probability that the collision causes the transition  $\hat{\jmath}-\hat{\jmath}'$ , wherein, at the same time, each contribution to the effectiveness of the latter,  $|\partial j'/\partial (\bar{q}_J/2\pi)|^{-1}$ , is weighted by  $D^K_{\delta',\delta}(\alpha\beta\gamma)$ , which describes the reorienting  $(\beta)$  and phase shifting  $(\alpha,\gamma)$  effectiveness of the collision, as discussed in Appendix C.

When the primitive semiclassical approximation breaks down, it can be replaced by a uniformlike approximation, and indeed we have used the latter in some other studies on rotational energy transfer. However, in the present instance, the contribution to the line shape of such events

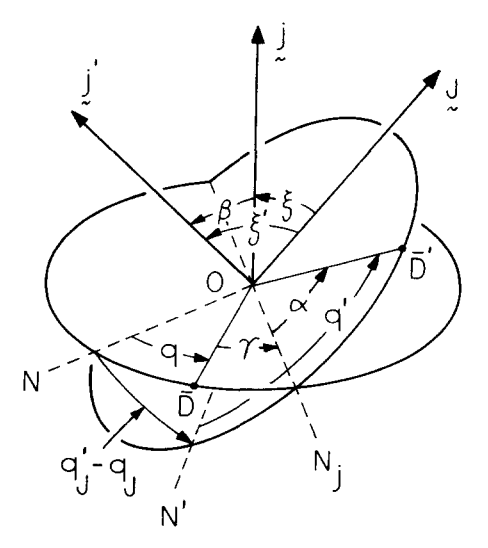


FIG. 2. Phase shift angles  $\alpha$  and  $\gamma$  and reorientation angle  $\beta$ . Here  $q=q_j-\omega_j t$  and  $q'=q'_j-\omega'_j t'$  are constants in the asymptotic regions of the trajectory. ON has the same significance as in Fig. 1, and ON is the corresponding line after collision.

was relatively small, and it sufficed for the present purposes to replace Eq. (2.11) by (2.16) for the event that the former expression exceeded unity:

$$P_{\hat{j}^{\bullet},\hat{j}} = \frac{\sum_{\mathbf{s},\mathbf{p},\bullet} |\partial_{j}^{\hat{j}'}/\partial(\overline{q}_{j}/2\pi)|^{-1} D_{\hat{s}^{\bullet},0}^{K}(\alpha\beta\gamma)}{\sum_{\mathbf{s},\mathbf{p},\bullet} |\partial_{j}^{\hat{j}'}/\partial(\overline{q}_{j}/2\pi)|^{-1}}$$
("elastic collision") . (2.16)

While the present calculations are concerned with pure rotational lines, we shall also make use of some experimental data on rotational-vibrational spectra. It is recalled from Part I that the half-widths,  $w_R$  and  $w_P$ , and the shifts,  $d_R$  and  $d_P$ , of the R and P branches, respectively, can be written in the form

$$w_{R} = BN \langle 1 - \sum C \cos(\alpha + \gamma + \eta_{v}) \rangle ,$$

$$w_{P} = BN \langle 1 - \sum C \cos(-\alpha - \gamma + \eta_{v}) \rangle ,$$

$$d_{R} = BN \langle \sum C \sin(\alpha + \gamma + \eta_{v}) \rangle ,$$

$$d_{P} = BN \langle \sum C \sin(-\alpha - \gamma + \eta_{v}) \rangle ,$$

$$(2.17)$$

where  $\eta_v$  is the vibrational phase shift;  $\eta_v$ , B, and C are obtained by comparing with the appropriate equations in Part I. They depend on v, b,  $\bar{q}_1$ ,  $\hat{J}$ ,  $\hat{J}$ , and the vibrational state. The phase shifts are usually small enough that the sines can be replaced by the angles themselves. When  $\eta_v$  is small,  $w_R$  and  $w_P$  are approximately equal to each other and to the w of the pure rotational spectra. When the shifts are small, one may set  $\sin(\alpha + \gamma \pm \eta_v) \cong \alpha + \gamma + \eta_v$ . Then  $\frac{1}{2}(d_R - d_P)$  is independent of  $\eta_v$  and is approximately equal to the d of the pure rotational spectra.

The comparison of Eq. (2.6) for the Wigner 6-j symbol with exact results and with the results based on the equation in Part I is given in Table I.

Finally, we note that if one wished to calculate  $\sigma_{fi,f'i'}^{K}$ , as in Ref. 16, one could do so using (2.8), (2.11), and the relation  $\sigma_{fi,f'i'}^{K} = \sigma_{if,i'f'}^{K*} = \sigma_{i'f',i'f'}^{K*}$ .

## III. RESULTS

For the CO-He, HCl-He, and HCl-Ar systems, a Buckingham exp-6 type potential (3.1), was used<sup>4,5</sup>:

$$V(R,\chi) = \frac{6\epsilon/\alpha}{1-6/\alpha} \exp\left[\alpha\left(1-\frac{R}{R_m}\right)\right] \left[1+r_1P_1(\cos\chi)+r_2P_2(\cos\chi)\right] - \frac{\epsilon}{1-6/\alpha} \left(\frac{R_m}{R}\right)^6 \left[1+a_1P_1(\cos\chi)\frac{R_m}{R}+a_2P_2(\cos\chi)\right] \ . \tag{3.1}$$

The potential parameters  $\epsilon$ ,  $R_m$ ,  $\alpha$ ,  $r_1$ ,  $r_2$ ,  $a_1$ , and  $a_2$  for those systems are given in Table II, and several parameters in the latter had been optimized<sup>4,5</sup> so as to give reasonable agreement of the experimental data with the theories that were used in Refs. 4 and 5.

For the OCS-He and OCS-Ar systems, the potential used<sup>4</sup> had an anisotropy in the attractive forces and no adjustable parameters, and is given by

$$V(R, \chi) = 4\epsilon \{ (\sigma/R)^{12} - (\sigma/R)^{6} [1 + a_{2}P_{2}(\cos\chi)] \} , \qquad (3.2)$$

where  $a_2$  in (3.2) is calculated from

$$a_2 = (\alpha' - \alpha'')/(\alpha' + 2\alpha'')$$
, (3.3)

where  $\alpha'$  and  $\alpha''$  are the longitudinal and transverse polarizabilities of the linear molecule. The values of  $\sigma$  and  $\epsilon$  calculated from the usual combination rules are  $\sigma=3.35$  Å and  $\epsilon=58.5$  °K, and  $\sigma=3.87$  Å and  $\epsilon=204$  °K for OCS-Ar, while  $a_2$  was 0.28 for OCS. <sup>16</sup> These values differ slightly from those used in Ref. 4. Since the potential (3.2) was of the form  $V(R,\chi)=V(R,\pi-\chi)$ , the first expression in Eq. (2.12) was utilized to calculate the cross section in this case.

The method used in the present paper for evaluating (2.3) and (2.8)–(2.11) was a standard Monte Carlo technique. In the initial studies (CO, HCl systems), the integrals over J and  $\overline{q}_l$  were evaluated by the so-called crude Monte Carlo procedure, while the integrals over v and l were evaluated by the stratified, group-sampled method. In the later studies (OCS systems), the integrals over J,  $\overline{q}_l$ , v, and b were evaluated by another Monte Carlo procedure. Is

The results for the linewidths, obtained from Eqs.

(2. 2)-(2. 4) and (2. 8)-(2. 16), are given in Table III, where the available experimental results are also given. The latter include both the half-widths of the microwave rotational lines, where available, and of the infrared rotational-vibrational lines. Comparison is also made there with the classical-type calculations of Gordon<sup>4</sup> for the CO, OCS, and HCl-He systems, and with the classical path calculations of Neilsen and Gordon<sup>5</sup> for the HCl-Ar system.

In reporting experimental widths and shifts, sometimes a Lorentzian is first used to fit the actual absorption coefficient  $\epsilon(\omega)$  instead of the reduced linewidth  $I(\omega)$ . <sup>18</sup> The resulting error is negligible for the infrared lines, but in the microwave case, the apparent shift would be reduced by about  $w^2/\omega_0$ , thus reducing somewhat the pure rotation figures in Table IV, as indicated there. The shifts  $d_R$  and  $d_P$  obtained from the R and P branches in infrared vibrational-rotational spectra were used to calculate  $\frac{1}{2}(d_R-d_P)$ , as noted in the previous section. These shifts are also reported in Table IV. In Table IV, a shift calculated by Neilsen and Gordon is also given.

To illustrate the velocity dependence of contributions

TABLE II. Potential energy parameters for HCl-Ar, HCl-He, and CO-He.

Molecule-atom system	$\epsilon \times 10^4$ (a.u.)	R <sub>m</sub> (a.u.)	α	$r_1$	$r_2$	$a_1$	$a_2$
CO-He a	1.073	6.63	12.0	0,70	0.70	0.30	0, 20
HCl-He <sup>a</sup>	1.893	6.25	12.0	0.36	0.10	0.18	0.10
HCl-Arb	6.374	7.21	13.5	0.35	0.65	0.30	0.09

Reference 4.

bReference 5.

TABLE III. Comparison of theoretical and experimental half-widths expressed as cross sections.

	Transition $j_i - j_i + 1$	Semiclassical half-width $(\mathring{A}^2)$	Classical or classical path	Experimental half-widths		
Molecule-atom system			half-width <sup>a</sup> (Ų)	Pure rot. $(\mathring{A}^2)$	$(\mathring{A}^2)^{\mathbf{b}}$	
СО-Не	10 → 11	26	31	•••	29	
HCl-Ar	$0 \rightarrow 1$	83	74	81 <sup>d</sup>	93	
	$4 \rightarrow 5$	32	31	$30^{d}$	38	
HC1-Не	$0 \rightarrow 1$	14	17	$14^{ exttt{d}}$	17	
	$1 \rightarrow 2$	13	• • •	• • •	14	
	4 → 5	12	14	$8^{\mathbf{d}}$	14	
	$5 \rightarrow 6$	11.5	• • •	•••	13	
	$9 \rightarrow 10$	8	10	• • •	10	
OCS-He	$0 \rightarrow 1$	33 <b>°</b>	• • •	• • •	• • •	
	$1 \rightarrow 2$	29 <sup>c</sup>	35	30°	• • •	
OCS-Ar	$0 \rightarrow 1$	143 <sup>c</sup>	• • •	• • •	• • •	
	$1 \rightarrow 2$	146 <sup>e</sup>	147	125 <sup>e</sup>	• • •	

<sup>&</sup>lt;sup>a</sup>The HCl-Ar system was treated (Ref. 5) by the classical-path-plus-quantum-internalstates method. All other systems in this column were treated (Ref. 4) by the classical method.

to the line broadening and shifting, some relevant results for the He-HCl (5 - 6 line) system are given in Figs. 3 and 4. Using stratified sampling in which all variables but the velocity v were integrated, the contribution of each velocity interval to the half-width and spectral shift is given in these figures.

## IV. DISCUSSION

The results in Table III for the half-widths are in quite reasonable agreement with those which Gordon and co-workers obtained by two quite different methods,

namely by a classical method for the CO, OCS, and HCl-He systems and by the quantum-internal-states-plus-classical-path method for the HCl-Ar system.

Both the experimental and calculated line shifts in Table IV are small except for the 0+1 line in the HCl-Ar case. The line shift obtained in Ref. 5 for that system is also given for comparison. There is an appreciable uncertainty in one of the two experimental shifts for the pure rotational lines, since it is not clear if they are computed from line shape vs  $\omega$  or reduced line shape vs  $\omega$  plots. An estimate of the possible correction

TABLE IV. Comparison of theoretical and experimental shifts expressed as cross sections.

	Transition $j_t \rightarrow j_f$	Semiclassical shift (Ų)	Previous calc.	Experimental shift		
Molecule—atom system			shifts $(\mathring{A}^2)$	Pure rot. $(\mathring{A}^2)$	$\frac{\frac{1}{2} (d_R - d_P)^{\mathbf{a}}}{(\mathring{\mathbf{A}}^2)}$	
CO-He	10 11	0.0	• • •	0.0		
HCl-Ar	$0 \rightarrow 1$	12.	8.1 <sup>b</sup>	31[-14] °	19	
	<b>4</b> → <b>5</b>	<b>-</b> 5.	• • •	0.0	3	
HC1-He	$0 \rightarrow 1$	1.3	•••	$1.8[-0.1]^{c}$	0.6	
	<b>1</b> → 2	0.4	• • •	0.0	0.4	
	<b>4</b> → 5	0.2	• • •	0.0	• • •	
	$5 \rightarrow 6$	0.2	• • •	0.0	•••	
	$9 \rightarrow 10$	0.1	•••	0.0	0.3	
OCS-He	$0 \rightarrow 1$	0.1 <sup>d</sup>	•••	0.0	• • •	
	$1 \rightarrow 2$	0.0 <sup>d</sup>	• • •	0.0	• • •	
OCS-Ar	0-1	-0,2 <sup>d</sup>	• • •	0.0	• • •	
	$1 \rightarrow 2$	-0.1d		0.0	• • •	

<sup>&</sup>lt;sup>a</sup>Reference 10.

 $<sup>{}^{</sup>b}w_{R}$  and  $w_{P}$  are the R- and P-branch half-widths, respectively, of the corresponding infrared lines given in Ref.  $9(j_{t} \rightarrow j_{t} + 1 \text{ and } j_{t} + 1 \rightarrow j_{t} \text{ for } w_{R} \text{ and } w_{P}, \text{ respectively})$ .  ${}^{c}$ Reference 16.

dReference 9.

eReference 11.

<sup>&</sup>lt;sup>b</sup>Reference 5.

<sup>&</sup>lt;sup>e</sup>The  $w^2/\omega_0$  term which would contribute to an apparent shift at a typical foreign gas pressure of 20 atm is indicated, with sign, in brackets, thus making the HCl-Ar systems have a possible shift of 17 Å<sup>2</sup>.

dReference 16.

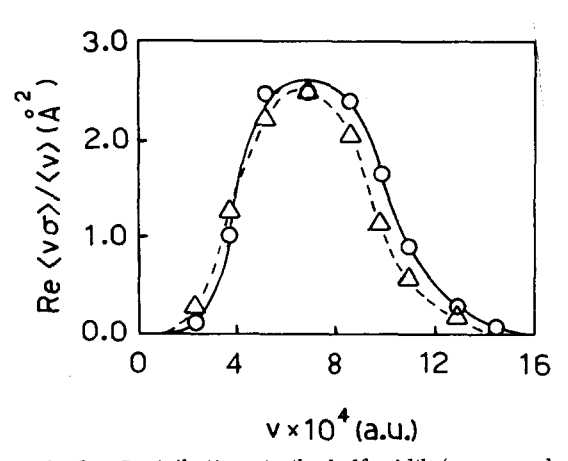


FIG. 3. Contributions to the half-width (expressed as cross sections) vs velocity are shown by (o) and are compared with a v-weighted velocity distribution versus velocity shown by ( $\Delta$ ). Each point (o) represents the contribution from a velocity increment  $\Delta v = 0.00015$  a.u. and is an average over all variables other than v.

 $(-w^2/\omega_0)$  is given in Table IV. The theoretical shifts themselves are less accurate than the theoretical widths.

The trends present in both the experimental and theoretical results include

- (i) a tendency for the linewidth to decrease with increasing  $\hat{j}$  in the  $j_t \rightarrow j_t$  lines,
- (ii) a marked decrease of the lineshift with increasing  $j_{\it i}$  , and
- (iii) a larger shift for the HCl systems, particularly the Ar one.

The present calculations indicate that effect (i) is primarily due to an increase in the probability of an elastic collision, with increasing  $\hat{j}$ : The higher the frequency of the internal motion, the more the principal rotational quantum number tends to be unchanged by collision, other things being equal. Effect (ii) is due to a decrease in magnitude of the typical phase shifts  $\alpha + \gamma$  at the higher j's, in part because of less distortion of the rotational motion by collision. Effect (iii) is reflected primarily in the larger values of  $\alpha + \gamma$  for the HCl systems. The low moment inertia molecule undergoes relatively larger distortions than a high moment of inertia molecule during the elastic collision. An analogous situation occurred in some collinear calculations of vibrational-translational energy transfer in an AB+C system: where the middle atom B was light it underwent large distortions during an elastic collision. 19 Analogously, Ar distorts the HCl rotation, and more than does He.

The effect of the dependence of inelastic collisions on the relative velocity of the collision partners may be seen from Figs. 3 and 4: The contributions to the half-width w and shift d from various velocity intervals (v,v+dv) are given as a function of v and compared with the velocity weighted distribution function  $v^3 \exp(-\mu v^2/2k_BT)$  which appears in the integrands. The parallelism is quite marked, but a specific velocity effect is also clear: The curve for the contribution to w is shifted to higher v's, while that for the contribution to d is shifted

to lower v's, relative to the v-weighted equilibrium distribution function. The higher v's are more effective in causing inelastic collisions and so contribute more to the width and, at the same time, since this  $P_{\hat{j},\hat{j}}$  is less, contribute less to the shift.

## V. CONCLUSION

The present results show that the semiclassical method yields reasonable results for the linewidths, both for the cases where a classical-like method had been used and also for the case (HCl-Ar at low j's) where a classical path plus coupled equations for quantum internal states method had been employed. As expected, the results for the lineshifts are less accurate than those for linewidths, but on the whole are reasonable.

## APPENDIX A: ADDENDA TO PART I

We have located the following typographical errors in Part I: In Eq. (3.3), for  $w_{j_i}$  and  $w_i$ , read  $\overline{w}_{j_i}$  and  $\overline{w}_i$ ; attention is also called to the note added in proof (p. 4387) which applied to Eq. (3.12) as well; in (3.13), for  $d_{\delta'\lambda}^R(\xi)$  read  $d_{\delta\lambda}^R(\xi)$ ; in (3.14), for  $i\delta'\gamma$  read  $i\delta\gamma$ ; in (3.15), for  $(\partial j'/\partial \overline{w}_j)_{w_i}$  read  $(\partial j'/\partial \overline{w}_j)_{w_i}^{-1}$ ; in (3.24) and the ensuing paragraph, the  $\langle v\sigma \rangle$ 's should be multiplied by N.

The angles  $\alpha$  and  $\gamma$  were mislabelled in Fig. 2. [They should be interchanged there and in Eqs. (5.3)–(5.8), second and seventh lines before (5.13), and in (5.13). ] This mislabelling would not have affected any numerical application of the basic equation, Eq. (3.12), since the  $D_{00}^{K}(\alpha\beta\gamma)$  in (3.12) was merely a symbol defined by (3.13), which did not explicitly contain  $\alpha\beta\gamma$ . Nevertheless, because of this error and because of the present incorporation of the angle  $\theta_2$  in the definition of the  $D_{00}^{K}(\alpha\beta\gamma)$  appearing in (3.12) of Part I, a proof given in the present Appendix C has been written to replace Appendix D of Part I. It is shown there that  $\alpha$  and  $\gamma$  are the angles given by the present Fig. 2.

Whereas in Fig. 1 of Part I we used a convention for  $q_J$  given by Whittaker, we now in the present Fig. 1 use that of Pars (cf. both in Ref. 15 of Part I) to conform with other studies here. Since only  $q_J - q_J'$  appears in the theory, there is no correction to any equation or discussion of Part I.

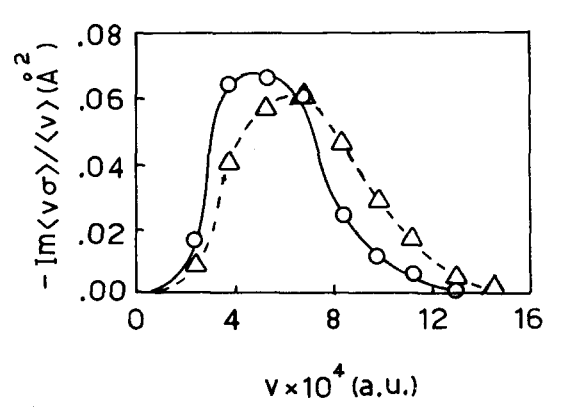


FIG. 4. Contribution to the shift (expressed as cross sections) vs velocity. Same notation as in Fig. 3.

#### APPENDIX B: SEVERAL PRACTICAL ASPECTS

The angles  $\bar{q}_f$ ,  $\bar{q}_f$ ,  $\bar{q}'_f$ ,  $\bar{q}'_f$ ,  $\bar{q}'_f$ ,  $w_E$ , and  $w'_E$  appearing in Part I, and used here, arise from a canonical transformation. As seen from Eqs. (3.8)-(3.10) of Part I, they are given by

$$\overline{q}_{j} = q_{j} - R\omega_{j}/v , \qquad \overline{q}'_{j} = q'_{j} - R'\omega'_{j}/v' \qquad (v < 0, v' > 0) ,$$

$$\overline{q}_{t} = q_{t} , \qquad \overline{q}'_{t} = q'_{t} ,$$

$$w_{F} - w'_{F} = t' - t - (R'/v') + (R/v) ,$$
(B1)

where  $\omega_j$  is  $\hat{j}/I$ ,  $\omega_j'$  is  $\hat{j}'/I$ , and both R and R' not only lie outside the interaction region, but also at a large enough R and R' that the (long range) centrifugal potential is negligible. If, instead, one begins a numerical integration of the trajectories at a point outside the interaction region but inside the "centrifugal potential region," the integration from that point to larger  $R(R=\infty)$  and  $R'=\infty$  can be performed analytically, by integrating the equations of motion using the unperturbed Hamiltonian  $H_0$ .

$$H_0 = (P_R^2/2\mu) + (\hat{j}^2/2I) + (\hat{l}^2/2\mu R^2)$$
 (at large R). (B2)

The variables  $q_i$ ,  $q_i$ , and R are canonically conjugate to  $\hat{j}$ ,  $\hat{l}$ , and  $P_R$ . Hamilton's equations of motion outside the interaction region yield

$$\begin{split} d\hat{j}/dt &= 0 \;, & dq_{j}/dt = \hat{j}/I \;, \\ d\hat{l}/dt &= 0 \;, & dq_{1}/dt = \hat{l}/\mu R^{2} \;, \\ d\hat{J}/dt &= 0 \;, & dq_{3}/dt = 0 \;, \\ dP_{R}/dt &= \hat{l}^{2}/\mu R^{3} \;, & dR/dt = P_{R}/\mu \;. \end{split} \tag{B3}$$

If we use x(t) or x(t'), where x is  $q_j$ ,  $q_1$ , R, or v, to denote the values of these varying quantities inside the centrifugal potential region to distinguish them from the values in (B1), the analytic integration of the equations in (B3) and introduction of them into (B1) yields

$$\overline{q}_j = q_j(t) - \omega_j R(t) v(t) / v^2 ,$$

$$\overline{q}'_i = q_i(t') - \omega_i' R(t') v(t') / v'^2 ,$$
(B4)

$$\bar{q}_{i} = q_{i}(t) + \sin^{-1}[\hat{l}/P_{R}(-\infty)R(t)],$$
 (B5)

$$\bar{q}_{1}' = q_{1}(t') + \sin^{-1}[\hat{l}'/P_{R}(\infty)R(t')],$$
 (B6)

$$w_E - w'_E = t' - t - R(t')v(t')/v'^2 + R(t)v(t)/v^2$$
 (B7)

The results in Eq. (2.12) can be obtained in the following way. The integral expression for the semiclassical S matrix is given by  $^{20}$ 

$$S_{j'l';jl}^{J} = \int_{0}^{2\pi} \frac{d\overline{q}_{l}}{2\pi} \int_{0}^{2\pi} \frac{d\overline{q}_{j}}{2\pi} \left| \partial(\overline{q}'_{j}\overline{q}'_{l}) / \partial(\overline{q}_{j}, \overline{q}_{l}) \right|^{1/2} \exp i\Delta ,$$
(B8)

where

$$\Delta = (\overline{j} - j')\overline{q}'_j + (\overline{l} - l')\overline{q}'_l - \int_{-J}^{\overline{J}} q_j(t)dj(t)$$

$$-\int_{-J}^{\overline{I}} q_i(t)dl(t) - \int_{-P_R}^{\overline{P}_R} R(t)dP_R(t) + \frac{1}{2}(l + l' + 1)\pi , \qquad (B9)$$

where  $q_j(t)$  indicates the instantaneous value of  $q_j$  along the trajectory, etc., and where  $\overline{j}$ ,  $\overline{l}$ , and  $\overline{P}_R$  denote the final values of j(t), l(t), and  $P_R(t)$  at the end of the trajectory.

The interaction potential  $V(R, \chi)$  depends on R and  $\chi$ , where  $\chi$  is the angle defined in Sec. II and is given by

$$\cos\chi = \cos q_{j} \cos q_{1} + \left[ (\hat{J}^{2} - \hat{l}^{2} - \hat{j}^{2}) \right] / 2\hat{j}\hat{l} \right] \sin q_{j} \sin q_{1} , \tag{B10}$$

where  $\chi$  lies in the  $(0,\pi)$  interval. A simultaneous decrease of  $q_j$  and  $q_i$  by  $\pi$  leaves (B10) unchanged. This decrease also leaves the Hamiltonian [given by the  $H_0$  in (B2) plus  $V(R,\chi)$ ] unchanged, and so leaves the j(t), l(t),  $\bar{j}$ , and  $\bar{l}$  in (B9) unchanged.  $q_j(t)$  and  $q_i(t)$  are decreased by  $\pi$ , however, and so thereby are  $q_j'$  and  $q_i'$ . Thus.

$$\Delta(\overline{q}_{i}' - \pi, \overline{q}_{i}' - \pi) = \Delta(\overline{q}_{i}', \overline{q}_{i}') - (j - j')\pi - (l - l')\pi. \tag{B11}$$

Before using this property, we first rearrange the domain of integration. If either  $\overline{q}_j$  or  $\overline{q}_l$  is changed by  $2\pi$ , the numerical value of neither  $\exp i\Delta$  nor the Jacobian in (B8) is changed. Thus, we can take the part of the integral over  $(\pi \leq \overline{q}_l \leq 2\pi)$ ,  $(0 \leq \overline{q}_j \leq \pi)$  and write it as the same integral over  $(\pi \leq \overline{q}_l \leq 2\pi)$ ,  $(2\pi \leq \overline{q}_j \leq 3\pi)$ . We can now write

$$\int_{0}^{2\pi} d\overline{q}_{1} \int_{0}^{2\pi} d\overline{q}_{j} = \int_{0}^{\pi} d\overline{q}_{1} \int_{0}^{2\pi} d\overline{q}_{j} + \int_{\pi}^{2\pi} d\overline{q}_{1} \int_{\pi}^{3\pi} d\overline{q}_{j} \cdots$$
(B12)

Now if the transformation  $(\overline{q}_l + \overline{q}_l - \pi, \overline{q}_j + \overline{q}_j - \pi)$  is introduced into the second integral on the right hand side of (B12) and if (B11) is used [the Jacobian in (B8) is unaffected, by the transformation, since  $\overline{q}'_i$  and  $\overline{q}'_j$  are merely also decreased by  $\pi$ ], we see that

$$\int_{0}^{\pi} d\overline{q}_{l} \int_{0}^{2\pi} d\overline{q}_{j} + \int_{\pi}^{2\pi} d\overline{q}_{l} \int_{0}^{2\pi} d\overline{q}_{j}$$

$$= \left[1 + \exp\{i(j'-j)\pi + i(l'-l)\pi\}\right] \int_{0}^{\pi} d\overline{q}_{l} \int_{0}^{2\pi} d\overline{q}_{j} \cdots$$
(B13)

Thus,  $S_{j'l',jl}^J$  vanishes if j'-j+l'-l is an odd integer. Thereby, for a given  $j,\ l$ , and j', it vanishes for one-half the l''s and its values for the other l''s are twice the values of the integral over the  $(0 \le \overline{q}_1 \le \pi)$ ,  $(0 \le \overline{q}_j \le 2\pi)$  domain.

We see from (B8) and (B13) that the product

$$S_{j_{i_{1}}, j_{i_{1}}}^{J_{i_{1}}} = S_{j_{i_{1}}, j_{i_{1}}}^{J_{i_{1}}},$$

which appears in Eq. (2.5) for  $\sigma_{i',j',if}^{K}$ , will vanish if either  $j_i-j_i'+l-l'$  or  $j_f-j_f'+l-l'$  is an odd integer. Thus, for it not to vanish, it suffices that (i)  $j_i-j_i'+l-l'$  be an even integer and (ii) that  $j_i-j_i'-(j_f-j_f')$  also be an even integer. This latter condition shows that  $\delta$  and  $\delta'$  can differ at most by an even integer. When condition (ii) is fulfilled, the  $S^{J_i}$   $S^{J_f}$  is 4 times larger than the value computed from the  $(0,\pi)(0,2\pi)$  domain in (B12). However, because of condition (i) only one-half the l''s appear, and so on the average, if one sums over all l''s, as in (2.5), the net result is only a factor of 2 greater than that given by evaluating the  $S^{J_i}$   $S^{J_f}$  in the  $[(0,\pi),(0,2\pi)]$  interval in (B13). When the 2 in  $d\overline{q}_i/2\pi$  in (B8) is taken into account, the value of s=1 which appears in (2.12) results.

We turn next to the verification of the first expression in (2.12). When the potential has the symmetry that

 $V(R,\chi)$  equals  $V(R,\pi-\chi)$ , the change of  $\overline{q}_1$  by an amount  $\pi$  causes no change in the Hamiltonian, and so there is no change in the values of j(t) and l(t). Introduction of this result into the integral in (B8) shows that

$$\int_{0}^{\pi} d\overline{q}_{i} \int_{0}^{2\pi} d\overline{q}_{j} = \left[1 + \exp i(l - l') \pi\right] \int_{0}^{\pi} d\overline{q}_{i} \int_{0}^{\pi} d\overline{q}_{j} \cdots \tag{B14}$$

Thus, one obtains from (B12)-(B14) the selection rule that l-l' is even. Since the selection rule that j'-j+l'-l is even was obtained earlier from (B13), the collisional selection rule that j-j' is even also follows. This selection rule was derived in an earlier article in this series of semiclassical papers. <sup>21</sup>

One sees from (B12)-(B14) that for even values of j-j',  $S^J$  thus equals 4 times the integral over the  $(\pi)^2$  domain in (B14). The contribution to  $S^{I_i}S^{J_i^*}$  is thus a factor of 16. Repeating the argument given earlier, summing over all the l''s instead of just half reduces this 16 to 8, and the 2 in the  $d\overline{q}_1/2\pi$  further reduces it to 4, thus accounting for the s=4 in the first expression in (2.12).

# APPENDIX C: PROOF OF EQ. (3.13) OF PART I

It will be noted from Fig. 2 that axes along j and  $O\overline{D}$  can be reached from axes along j' and  $O\overline{D}$ ' via six successive rotations or via three, and we wish to obtain a relation between them.

Conventionally, three successive Euler angle rotations are performed by rotating through an angle  $\alpha_0$  about the z axis of a set of axes S, then rotating through an angle  $\beta_0$  about the y' axis of the new set of axes S' produced by the first rotation, and then rotating through an angle  $\gamma_0$  about the z'' axis of the set of axes S'' produced by the second rotation. This series of rotations can be described by the operator  $D_{z'}(\gamma_0)D_{y'}(\beta_0)D_{z}(\alpha_0)$ . Alternatively, using the argument in Ref. 22, this rotation can be described as a rotation  $\gamma_0$  about the z axis, followed by a rotation  $\beta_0$  about the y axis, and finally by a rotation  $\alpha_0$  about the z axis, all in the original frame S. Hence, as in Ref. 22,

$$D_{\mathbf{z}'} \cdot (\gamma_0) D_{\mathbf{y}'} \cdot (\beta_0) D_{\mathbf{z}} (\alpha_0) = D_{\mathbf{z}} (\alpha_0) D_{\mathbf{y}} (\beta_0) D_{\mathbf{z}} (\gamma_0)$$

$$= D(\alpha_0 \beta_0 \gamma_0) , \qquad (C1)$$

where the usual symbol  $D(\alpha_0\beta_0\gamma_0)$  for the rotation operator has been introduced.  $D_s(\alpha_0)D_s(\beta_0)D_s(\gamma_0)$ , rather than the left hand side of (C1), is used to compute the rotation matrix elements  $D^j_{mm^*}(\alpha\beta\gamma)$ . Omitting the subscripts on the  $\alpha$ ,  $\beta$ ,  $\gamma$ , for brevity, we have (Ref. 12, p. 55)

$$D_{mm^{\bullet}}^{f}(\alpha\beta\gamma) = e^{i\,m\,\alpha}\,d_{mm^{\bullet}}^{f}(\beta)\,e^{i\,m^{\bullet}\gamma} \quad . \tag{C2}$$

Similarly, one may apply the rotations  $\alpha_2 \beta_2 \gamma_2$ , followed by  $\alpha_1 \beta_1 \gamma_1$ , denoting the successive sets of axes by S,  $S^{(1)}$ ,  $S^{(2)}$ ,  $S^{(3)}$ ,  $S^{(4)}$ , and  $S^{(5)}$ ; one rotates through  $\alpha_2$  about z, then successively through  $\beta_2$  about  $z^{(1)}$ ,  $\gamma_2$  about  $z^{(2)}$ ,  $\alpha_1$  about  $z^{(3)}$ , ' $\beta_1$  about  $z^{(4)}$ , and  $\gamma_1$  about  $z^{(5)}$ . Using a proof which parallels that in Ref. 22, but now applied to six rotations instead of three, it can be shown that

$$\begin{split} D_{z(5)}(\gamma_1)D_{y(4)}(\beta_1)D_{z(3)}(\alpha_1)D_{z(2)}(\gamma_2)D_{y(1)}(\beta_2)D_{z}(\alpha_2) \\ &= D_{z}(\alpha_2)D_{y}(\beta_2)D_{z}(\gamma_2)D_{z}(\alpha_1)D_{y}(\beta_1)D_{z}(\gamma_1) \\ &= D(\alpha_2\beta_2\gamma_2)D(\alpha_1\beta_1\gamma_1) \quad . \end{split}$$
 (C3)

When the final result of the series of rotations on the left hand side of (C1) is the same as that on the left hand side of (C3), they may be equated and so, therefore, may the right hand sides. Thus,

$$D(\alpha_2\beta_2\gamma_2)D(\alpha_1\beta_1\gamma_1)=D(\alpha_0\beta_0\gamma_0) . (C4)$$

Computing matrix elements and introducing the closure relation, one obtains the well-known expression (Ref. 12, p. 63)

$$\sum_{\lambda^{2}=K}^{K} D_{\delta'\lambda}^{K}(\alpha_{2}\beta_{2}\gamma_{2}) D_{\lambda\delta}^{K}(\alpha_{1}\beta_{1}\gamma_{1}) = D_{\delta'\delta}^{K}(\alpha_{0}\beta_{0}\gamma_{0}) . \tag{C5}$$

In our case it is important to note that  $D(\alpha_2\beta_2\gamma_2)$   $D(\alpha_1\beta_1\gamma_1)$  can be interpreted as the left hand side of (C3). If one chooses an axis system S before the first rotation such that the y axis lies down  $O\overline{D}'$  of Fig. 2 and the z axis lies down j' of the same figure, the six rotations which can be executed to bring the final axis system into a position such that the final y axis lies down  $O\overline{D}$  and the z axis lies down j are seen from Fig. 2 to be -q',  $-\xi'$ ,  $-q'_J$ ,  $q_J$ ,  $\xi$ , and q, respectively. This net rotation brings the above axis system containing  $O\overline{D}'$  into  $O\overline{D}$  and also corresponds to executing three rotations through the angles  $-\alpha$ ,  $-\beta$ , and  $-\gamma$  in Fig. 2. In either case, this net rotation of axes is equivalent to rotating a field point  $\overline{D}$  into  $\overline{D}'$ .

We now apply (C5). The  $D_{0'0}^{K}(\alpha\beta\gamma)$  appearing in (2.11) is the same as the right hand side (rhs) of (3.13) of Part I, but now including the  $\exp(i\theta_2)$  term in its definition. We thereby have from (3.13) of Part I,

$$D_{\delta^{\prime}\delta}^{K}(\alpha\beta\gamma)\ln(2.11) = \sum_{k=-K}^{K} e^{i(\theta_{1}+\theta_{2})} d_{\delta\lambda}^{K}(\xi) d_{\delta^{\prime}\lambda}^{K}(\xi^{\prime}) , \quad (C6)$$

where  $\theta_1 + \theta_2$  is found from Sec. III of Part I to be given by

$$\theta_{1} + \theta_{2} = \overline{q}_{j}' \delta' - \overline{q}_{j} \delta + w_{E}(E_{i} - E_{f}) - w_{E}'(E_{i}' - E_{f}') + (q_{J}' - q_{J}) \lambda .$$
(C7)

The  $\overline{q}$ 's are the  $2\pi \overline{w}$ 's in Part I. When  $E_i - E_f$  equals  $E_i' - E_f'$  only  $w_E - w_E'$  appears in (A2) and is given by (B7). All of the calculations in the present paper involved i = i', f = f', and hence  $E_i - E_f = E_i' - E_f'$ .

We wish to show that the lhs of (C6) defines a rotation matrix, with angles  $\alpha\beta\gamma$  given by Fig. 2. First, according to Eqs. (C6) and (C7), we have

lhs of (C6)

$$= \sum_{\lambda=-K}^{K} \left[ e^{-i\,q\,\delta} d_{\delta\lambda}^{K}(\xi) e^{-i\,q\,j\lambda} \right] \left[ e^{i\,q'\,\delta'} d_{\delta'\lambda}^{K}(\xi') e^{i\,q'j\lambda} \right] , \qquad (C8)$$

where<sup>23</sup>

$$q' = q'_j - w'_j t'$$
,  $q = q_j - w_j t$ ,  
 $w'_j = E'_j - E'_i$ ,  $w_j = E_j - E_i$ . (C9)

Using the d- and D matrix relations (Ref. 12, p. 60) and using (C5), Eq. (C8) may be manipulated to give (C10).

Here, we have made the following identification for  $\alpha_2$ ,  $\beta_2$ ,  $\gamma_2$ ,  $\alpha_1$ ,  $\beta_1$ ,  $\gamma_1$ ,  $\alpha_0$ ,  $\beta_0$ , and  $\gamma_0$  in (C5): -q',  $-\xi'$ ,  $-q'_J$ ,  $q_J$ ,  $\xi$ , q,  $-\alpha$ ,  $-\beta$ , and  $-\gamma$ , respectively. <sup>24</sup> Thus,

lhs of (C6)=
$$\sum_{\lambda}D^K_{-\delta'-\lambda}(-\,q^{\,\prime},\,-\,\xi^{\,\prime},\,-\,q^{\,\prime}_{J})D^K_{-\lambda-\delta}(q_{J}\,,\,\xi\,,\,q\,)$$

$$=D_{-\delta'-\delta}^{K}(-\alpha,-\beta,-\gamma)=D_{\delta'\delta}^{K}(\alpha\beta\gamma) , \qquad (C10)$$

which shows that the lhs of (C6) equals  $D_{\delta^*\delta}^K(\alpha\beta\gamma)$  and thus justifies using this symbol for it in (2.11).

For purposes of additional interpretation of the rotations in (C10), it is convenient to use a more conventional notation (e.g., Ref. 25) for the D matrices. In terms of this notation, which we shall denote by  $\overline{D}$ , we have<sup>25</sup>

$$D_{\delta,\delta}^{K}(\alpha\beta\gamma) \equiv \overline{D}_{\delta,\delta}^{K}(-\alpha, -\beta, -\gamma) . \tag{C11}$$

Rotation of the axes through an angle  $\varphi$  is achieved in this more common notation by the operator  $\exp(-i\varphi J_x)$ , where  $J_x$  is the operator for the z component of the angular momentum:  $\overline{D}_{\mathfrak{d}'\mathfrak{d}}(-\alpha,-\beta,-\gamma)$  in (C11) is thus the matrix element for rotating the axes which lie along  $\mathbf{j}'$  and  $O\overline{D}'$  in Fig. 2 into ones which lie along  $\mathbf{j}$  and  $O\overline{D}$ . It is also, thereby, the matrix element for transforming a dipole  $O\overline{D}$  into  $O\overline{D}'$  by a collision, since rotation of the axes is equivalent to rotation of the system in the opposite sense.

- Proceedings No. 11, edited by J. Kestin (American Institute of Physics, New York, 1973), p. 51.
- <sup>9</sup>H. A. Gebbie and N. W. B. Stone, Proc. Phys. Soc. **82**, 309 (1963).
- <sup>10</sup>D. H. Rank, D. P. Eastman, B. S. Rao, and T. A. Wiggins, J. Mol. Spectrosc. **10**, 34 (1963).
- <sup>11</sup>K. Srivastava and S. L. Srivastava, J. Chem. Phys. 41, 2266 (1964).
- <sup>12</sup>A. R. Edmonds, Angular Momentum in Quantum Mechanics (Princeton U. P., Princeton, NJ, 1960), 2nd ed., Appendix 2 p. 122,
- <sup>13</sup>The degeneracy term comes from the evaluation of  $|\langle j_f || \mu || j_t \rangle|^2$ .
- <sup>14</sup>J. D. Doll and W. H. Miller, J. Chem. Phys. 57, 5019 (1972); W. H. Miller and A. W. Raczkowski, Chem. Soc. Faraday Discuss. 55, 45 (1973).
- <sup>15</sup>Reference 12, pp. 94-95.
- <sup>16</sup>W.-K. Liu and R. A. Marcus, J. Chem. Phys. (submitted), (a) a study on microwave transient phenomena and on line shapes, (b) applications.
- <sup>17</sup>The trajectories themselves were calculated using a standard Hamming's modified predictor—corrector method. [A. Ralston and H. S. Wilf, Mathematical Methods for Digital Computers (Wiley, New York, 1960), pp. 55–109)]. Generally, about 100 sample points in the  $(\overline{q}_1, \hat{J}, v, b)$  space were used to find the major contribution to the width and shift. (There were typically about two stationary phase points per sample point.) Often, about 100 more points were used to insure convergence of the result when the stratified sampling procedure was used. When instead an importance—sampled Monte Carlo procedure was used for v, b, and  $\hat{J}$ , and a crude Monte Carlo for  $\overline{q}_1$ , a total of about 100 sample points were used.
- <sup>18</sup>The relationship between the actual absorption coefficient measured in experiment and the reduced line shape is given in Ref. 4 [Eq. (2.1)].
- <sup>19</sup>J. D. Kelley and M. Wolfsberg, J. Chem. Phys. **44**, 324 (1966); M. Attermeyer and R. A. Marcus, J. Chem. Phys. **52**, 393 (1970).
- <sup>20</sup>E.g., R. A. Marcus, J. Chem. Phys. **56**, 311 (1972), Eqs. (7.7)-(7.8). The Jacobian for transforming from initial to final variables was also used.
- <sup>21</sup>R. A. Marcus, J. Chem. Phys. **54**, 3965 (1971).
- <sup>22</sup>Reference 12, \$1.3, p. 8.
- <sup>23</sup>For the case that  $E_i E_f \neq E_i' E_f'$ , the individual values of  $w_E$  and  $w_E'$  appear rather than merely  $w_E w_E'$ . (Note, however, that differences in  $E_i E_f$  and  $E_i' E_f'$  are neglected in the impact approximation.)<sup>2</sup> We use the values of  $w_E$  and  $w_E'$  at zero time (which defines thereby the time at which collision occurs —it is instantaneous in the impact approximation). From Eqs. (C9)–(C11) of Part I, these values of  $w_E$  and  $w_E'$  are found to be (R'/v') t' and (R/v) t, respectively.
- <sup>24</sup>Thereby, the S, ...,  $S^{(5)}$  frames involved in (C3) occupy the following positions for their z and y axes, respectively, in Fig. 2: j' and  $O\overline{D}'$  for S; j' and ON' for  $S^{(1)}$ ; J and ON' for  $S^{(2)}$ ; J and a point not shown but which lies in the plane of the triangle ONN' and on the OX axis of Fig. 1 for  $S^{(3)}$ ; J and ON for  $S^{(4)}$ ; j and ON for  $S^{(5)}$ . The frame finally ends up at what we could call  $S^{(6)}$ , with its z and y axes being j and  $O\overline{D}$ .
- <sup>25</sup>D. M. Brink and G. R. Satchler, Angular Momentum (Clarendon, Oxford, England, 1968), 2nd ed., p. 21.

<sup>\*</sup>Supported in part by a grant from the National Science Foundation.

<sup>&</sup>lt;sup>1</sup>See reviews by H. Rabitz, Ann. Rev. Phys. Chem. 25, 155 (1974); J. J. M. Beenaker, H. F. P. Knaap, and B. C. Sanctuary, in *Transport Phenomena* 1973, AIP *Conference Proceedings*, No. 11, edited by J. Kestin (American Institute of Physics, New York, 1973), p. 21; R. G. Gordon, Adv. Magn. Reson. 3, 1 (1968); R. G. Gordon, W. Klemperer, and J. I. Steinfeld, Ann. Rev. Phys. Chem. 19, 215 (1968); G. Birnbaum, Adv. Chem. Phys. 12, 487 (1967).

 <sup>&</sup>lt;sup>2</sup>D. E. Fitz and R. A. Marcus, J. Chem. Phys. 59, 4380 (1973) (Part I). (For addenda see the present Appendix A.)
 <sup>3</sup>We are indebted to Mr. Wing-Ki Liu of this laboratory for the OCS results.

<sup>&</sup>lt;sup>4</sup>R. G. Gordon, J. Chem. Phys. 44, 3083 (1966).

<sup>&</sup>lt;sup>5</sup>W. B. Neilsen and R. G. Gordon, J. Chem. Phys. **58**, 4131 (1973); J. Chem. Phys. **58**, 4149 (1973).

<sup>&</sup>lt;sup>6</sup>An interesting theoretical treatment using a "centrifugal" approximation has been used by W. A. Cady, J. Chem. Phys. **60**, 3318 (1974) to calculate half-widths of  $j=1 \rightarrow 2$  OCS lines broadened by He and Ar. Using the potential in Ref. 4, he obtained reasonable values.

<sup>&</sup>lt;sup>7</sup>For comments on classically calculated line shifts see Ref. 4, p. 3089 and R. G. Gordon and R. P. McGinnis, J. Chem. Phys. 55, 4898 (1971), p. 4904.

<sup>&</sup>lt;sup>8</sup>R. G. Gordon, in Transport Phenomena-1973, AIP Conference